

# The effects of concentration on partitioning of flexible chains into pores

Tomas Bleha\*, Peter Cifra\* and Frank E. Karasz†

Department of Polymer Science and Engineering, University of Massachusetts,  
Amherst, MA 01003, USA

(Received 5 May 1989; revised 5 September 1989; accepted 9 September 1989)

Equilibrium partitioning between bulk solution and pores was investigated by computer experiment using the Monte Carlo technique. In a multichain athermal system, self-avoiding walks of up to 60 steps were generated on a simple cubic lattice with variable pore size and chain concentration. The results demonstrate that the constraints imposed by the pores and/or neighbouring chains reduce the chain entropy. The entropy related parameter, the partition coefficient  $K$  (the equilibrium pore-to-bulk concentration ratio) increases linearly with bulk concentration  $\phi$ . A maximum concentration dependence of  $K$  was found for large pores characterized by a coil-to-pore dimension ratio  $\lambda$  of about 0.1–0.3. In this range the increase in bulk concentration brings about a dramatic enhancement of partitioning into pores. The results of computer experiments are compared with predictions of hard-sphere solutes theory and with static and gel-chromatographic measurements of the partitioning equilibrium. The implications of the concentration-dependent coefficient  $K$  for hindered transport of flexible polymers inside pores are briefly discussed.

(Keywords: self-avoiding walks; Monte Carlo simulations; steric partitioning; gel chromatography; hindered transport)

## INTRODUCTION

The distribution of molecules between a porous medium and bulk solution is characterized by the distribution coefficient  $K$ , given as the ratio of the average concentration inside the pore to the equilibrium concentration in the bulk phase,  $K = C_p/C$ . In the ideal case of purely steric partitioning, the pore walls behave as hard walls. The geometric excluded volume adjacent to the pore walls that is not accessible to the centre of solute particles due to their finite size is responsible for the partitioning. In infinitely dilute solution the partitioning coefficient  $K_0$  is determined only by interactions between pores and single isolated particles.

The theoretical description of steric partitioning is at present focused on the dependence of the partition coefficient on the size and shape of the solute and the pore. For spherical solutes analytical expressions for the coefficient  $K$  have been determined for pores of various idealized geometries such as spheres, slits, cylinders or pores with elliptical or rhomboidal cross sections<sup>1–3</sup>. Giddings *et al.*<sup>1</sup> have presented a general formulation for the partitioning of rigid particles of an arbitrary shape. For flexible polymers, the partitioning of random flight chains between the bulk solution and pores of various sizes was analysed by Casassa<sup>4</sup> using a differential equation analogous to that used to describe heat conduction. Expressions were derived relating the coefficient  $K$  to  $\lambda$ , the ratio of the characteristic dimensions of the coil,  $R_g$ , to a pore  $a_p$ , where  $R_g$  is the radius of gyration of the polymer chain. This approach was later extended to star-branched polymers<sup>5</sup>. However, Casassa's<sup>4</sup> fundamental results are strictly valid only for flexible, infinitely long ideal chains under theta conditions in infinitely dilute solution.

At finite concentration solute-solute interactions within the pores also have to be considered and the partition coefficient then becomes concentration dependent. Glandt<sup>2,3</sup> was the first to compute the effect of concentration on the coefficient  $K$  for purely steric hard sphere-hard wall interactions for pores of various shapes. He used a virial-type expansion of the coefficient  $K$  to the power of the bulk solution concentration

$$K = K_0 + \alpha_1\phi + \alpha_2\phi^2 \quad (1)$$

where  $\phi$  is the volume fraction of the solute in bulk solution. The calculation<sup>2,3</sup> predicted that the coefficient  $K$  would increase with the bulk concentration because the pore walls induced the accumulation of solute near the wall periphery even in the absence of attractive solute-wall forces. A similar theory<sup>6</sup> for the concentration dependence of the coefficient  $K$  was developed independently for rigid spherical macromolecules in both cylindrical pores and slits and was extended to systems containing charged solutes within pores. The effects of electrostatic interactions on the partitioning of spherical solutes at finite concentration have been discussed in more detail in reference 7. There is, unfortunately, no analytical theory available at present for the concentration dependence of the coefficient  $K$  for flexible polymers which would extend Casassa's results<sup>4,5</sup> to finite concentrations.

Monte Carlo simulations (MC) on a lattice represent an attractive alternative to the analytical theories of partitioning for flexible chains<sup>8–10</sup>. Using this technique the essential result of the theory of partitioning, the behaviour of  $K$  as a function of  $\lambda$ , can be evaluated for a variety of situations where the analytical solution does not exist. For example Monte Carlo studies<sup>9</sup> have demonstrated that chain flexibility plays a prominent role in partitioning and that the coefficient  $K$  for chains with finite segment length may be substantially higher than that for chains with infinitesimally short segments. Our

\* Permanent address: Polymer Institute, Slovak Academy of Sciences, 842 36 Bratislava, Czechoslovakia

† To whom correspondence should be addressed

previous simulations<sup>10</sup> focused on the effect of the solvent on the partition equilibrium and it was found that  $K$  versus  $\lambda$  for a cubic pore was only slightly affected by the quality of solvent. In the present work the Monte Carlo technique is applied to investigate the concentration dependence of the coefficient  $K$  for flexible chains with a variable number of segments  $N$  in equilibrium with cubic pores of variable size. This problem is of considerable interest to both theoreticians and experimentalists in connection with the concentration effects observed in static partitioning<sup>11</sup>, gel chromatography<sup>12-14</sup>, and hindered transport of flexible molecules in porous materials<sup>15,16</sup>. The results reported in this paper corroborate and extend our previous conclusions<sup>17</sup> in that the partition coefficient  $K$  increases linearly with bulk concentration and that partitioning in the larger size range of the pores may be dramatically enhanced.

## METHOD OF CALCULATION

The procedure for generating self-avoiding walks on a simple cubic lattice with restrictions imposed by cubic pores is described in previous papers<sup>10,17</sup>. Chains comprising 20, 40 and 60 segments were generated in a cubic lattice of size  $L$  equal to 8 to 65 lattice sites. The scanning generation procedure was used<sup>18</sup> in which the lattice is filled by the addition of one chain at a time avoiding double occupancy of sites. Configurations were constructed by adding monomers according to a step-by-step procedure.

An athermal system with zero intersegmental energy in which the partition coefficient  $K$  is determined only by the entropic term:  $\ln K = (S_{cf} - S_f)/R = \Delta S/R$ , was used in the simulations. The entropy of free chains ( $S_f$ ) and chains confined by pores ( $S_{cf}$ ) at a concentration  $\phi$  expressed as volume fraction was obtained in two steps. First, a box representing a pore was filled by chains up to the required  $\phi$ . Then an extra trial chain was added to a multichain assembly<sup>19</sup> and the number of possible configurations of this chain  $W_N$  at a given  $\phi$  was determined. A site occupied by the first segment of a chain was selected at random from unoccupied states and the number of its unoccupied neighbour sites  $v_2$  was counted. The second element of the extra  $N$ -mer chain was assigned randomly to any of the  $v_2$  sites. The third segment was randomly assigned to any of  $v_3$  free sites adjacent to the second segment and so on. This procedure was repeated many times for one multichain sample and also for many samples. The number of configurations per chain was then given by

$$W_N = (1 - \phi) \left\langle \prod_{i=2}^N v_i \right\rangle \quad (2)$$

Averages were calculated for 3000–15 000 trial chains. Volume fractions of up to about 0.25, 0.20 and 0.15 were used for chains with 20, 40 and 60 segments, respectively.

The above method was used to generate a multichain system representing either the bulk solution in which periodic boundary conditions in the box were assumed or chains within a pore with reflecting but otherwise inert walls. In the latter case, the outer layers of the box (walls) were assumed to be inaccessible before filling the pore with chains. To ensure the same volume, different box sizes were used for confined and unconfined systems,  $L_{cf} = L_f + 2$ .

The mean square end-to-end distance of the chain  $\bar{r}_2$  and the radius of gyration  $R_g$  were calculated in an analogous way, by averaging the self-avoiding walks. These quantities as well as the pore size  $a_p = L/2$  are expressed in the units of the lattice modulus.

## RESULTS AND DISCUSSION

The molecule-to-pore size ratio  $\lambda = R_g/a_p$  is usually employed as a measure of chain confinement by a pore. The effective partitioning of macromolecules takes place in the range of large pores for which the radius of gyration is much smaller than the pore size. While  $a_p$  can be considered as a fixed parameter, the selection of an appropriate value of  $R_g$  to be used in  $\lambda$  is more ambiguous. Traditionally, the radius of gyration  $R_g^0$  corresponding to a free chain in an infinitely dilute system is used as a measure of coil size. However, the confinement of a chain in a pore brings about a reduction in coil size. A typical example of this type of behaviour is shown in Figure 1 from calculations for a single chain with 100 segments confined in a box of size  $L$  under conditions simulating the theta state. It is evident that the considerable reduction in coil size occurs much earlier than at the point where the size of a free chain matches the pore size, i.e. at  $2R_g^0 = L$ . The dimensions of a confined coil at this point amount to only about 40% of the size of the free chain. The data in Figure 1 converge to the values calculated previously<sup>20</sup> for a free chain as the pore constraint is gradually relieved.

The problem of finding appropriate values of  $R_g$  is further compounded at finite concentrations since an increase in concentration reduces the coil size, a phenomenon well documented in the literature both by experiments<sup>21</sup> and by Monte Carlo simulations<sup>19</sup>. Both factors which reduce the coil size, concentration and confinement by the pore walls, are similar and originate from the diminished number of configurations available to a reference chain. Despite these ambiguities, to facilitate the comparison with previous partitioning studies we will

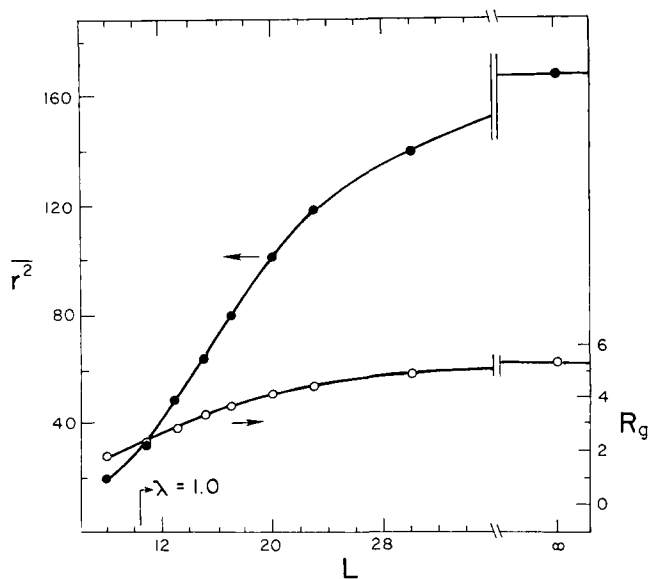


Figure 1 The end-to-end distance  $\bar{r}_2$  and the radius of gyration  $R_g$  of a chain with 100 segments as a function of the pore size  $L$  simulated in a theta system (with the intrasegmental energy parameter  $F = 0.26$ , ref. 10); results for unconfined chains are from reference 20

**Table 1** The concentration dependence of the partition coefficient  $K$  according to equation (1). Simulations obtained for an athermal system of chains with a number of segments  $N$  at a coil-to-pore ratio  $\lambda = R_g^0/a_p$ .  $K_0$  and  $K(0.1)$  are the partition coefficients at infinite dilution and bulk concentration  $\phi = 0.1$ , respectively

$N$	$R_g^0$	$\lambda$	$\alpha_1$	$K_0$	$K(0.1)$
20	2.41	0.08	1.54	0.82	0.98
		0.11	1.68	0.77	0.93
		0.16	2.04	0.64	0.84
		0.19	1.64	0.59	0.75
		0.24	1.18	0.51	0.63
		0.32	0.94	0.39	0.49
		0.48	0.41	0.20	0.24
		0.69	0.07	0.06	0.07
40	3.68	0.80	0.00	0.03	0.03
		0.15	3.50	0.65	1.00
		0.25	2.33	0.46	0.69
		0.37	1.48	0.28	0.43
		0.61	0.18	0.09	0.10
		0.74	0.08	0.03	0.03
60	4.73	0.92	0.0	0.0	0.0
		0.20	1.55	0.56	0.72
		0.27	1.31	0.43	0.56
		0.47	0.80	0.17	0.25
		0.79	0.05	0.02	0.02
		0.94	0.0	0.0	0.0

henceforth use the value  $R_g^0$  computed for a single chain to express the ratio  $\lambda$  (Table 1).

Both the bulk concentration and the pore confinement strongly affect the averaged thermodynamic functions of the chains. The dependence of the entropy of free chains and that of chains inside a pore as a function of the bulk phase volume fraction is shown in Figures 2 and 3 for chains of length 20, 40 and 60 at different values of  $\lambda$ . In agreement with our previous study for single chains<sup>10</sup> the entropy is strongly reduced by the confinement of chains inside pores and this trend is further enhanced by an increase in concentration. For small pores the very low concentrations within cannot be probed by computations because even the most dilute systems with a single chain in a box correspond to a rather high value of volume fraction  $\phi$ . The data in this region can be derived only by extrapolation of the curves obtained at higher concentrations. Figures 2 and 3 also show data for unconstrained chains reported for an analogous multi-chain system by Okamoto<sup>19</sup>. Both sets of data agree very well for chains with  $N=20$ , however, for longer chains data from reference 19 predict a slightly sharper decrease in entropy with concentration than is indicated in our simulations.

Because in athermal systems the partition coefficient is proportional to the change in entropy  $S_{cf} - S_f$ , the relative difference in the rate of decrease of the entropy curves for confined chains relative to those for free chains determines the concentration dependence of the partition coefficient. An identical rate of decrease of these curves indicates that  $K$  is independent of concentration. As an example, the above differences evaluated for chains with 20 and 40 segments are plotted in Figures 4 and 5. The computed points in these figures can be approximated by straight lines. An analogous linear dependence of the coefficient  $K$  on the bulk volume fraction  $\phi$  was also found for chains with 60 segments. Evidently, in the range of concentration studied, the first two terms in equation (1) are sufficient to describe the concentration dependence of the coefficient  $K$ . Although no data are available for

the coefficient  $K$  at high  $\phi$  and low  $\lambda$ , it is likely that  $K$  converges to unity but does not exceed it.

The slopes  $\alpha_1$  and intercepts  $K_0$  for the systems studied are listed in Table 1. The parameter  $K_0$ , determined by extrapolation, refers to partitioning in infinitely dilute systems and its value may be different from that obtained

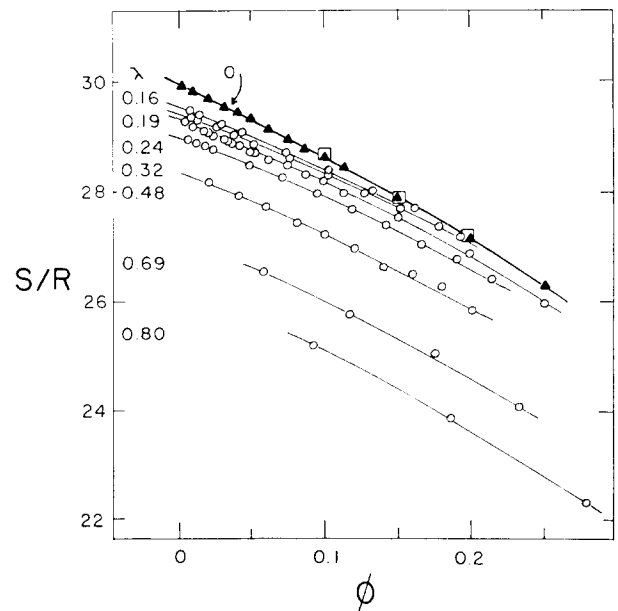


**Figure 2** The entropy of free chains ( $\blacktriangle$ ) and of confined chains as a function of the bulk volume fraction  $\phi$  at specified coil-to-pore ratios ( $\lambda$ ) in an athermal system for chains with  $N=20$ . The open squares show data obtained for free chains from reference 19

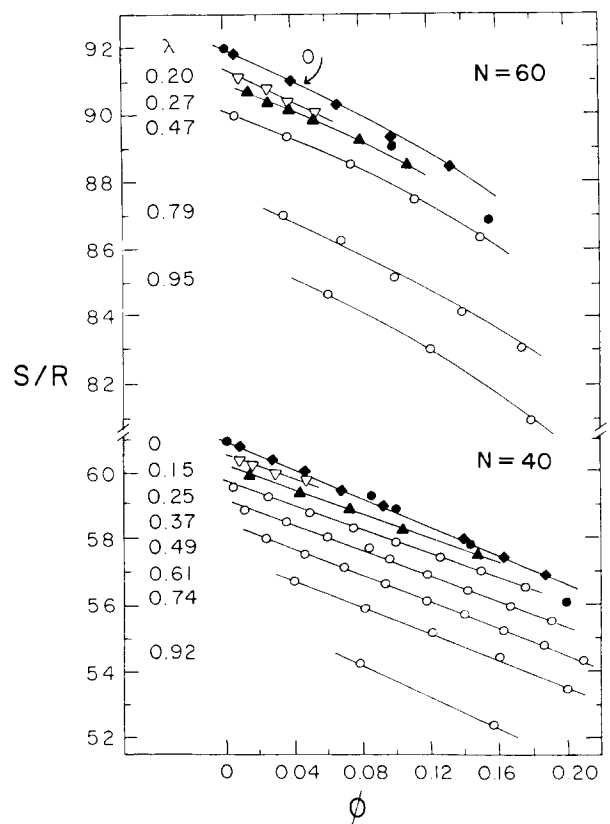


**Figure 3** The entropy of free chains ( $\blacklozenge$ ) and of confined chains as a function of the bulk volume fraction  $\phi$  at specified coil-to-pore ratios ( $\lambda$ ) in an athermal system for chains with  $N=40$  and  $N=60$ . The full circles show data obtained for free chains from reference 19

by computation for the most dilute system, that containing a single chain. For comparison Table 1 also lists the values of  $K(0.1)$  corresponding to the partition coefficient at concentration of 10 vol%. The magnitude of the slope  $\alpha_1$  is a sensitive function of the confinement parameter  $\lambda$ . In the region of large pores at  $\lambda$  of about 0.1–0.4, the concentration effect becomes pronounced. It is seen from Figures 4 and 5 and from Table 1 that the concentration effect becomes negligible for small pores at  $\lambda$  greater than about 0.7. As  $\lambda \rightarrow 0$  the concentration effect also vanishes as the pore confinement becomes undetectable. These features of the variation of the slope  $\alpha_1$  as a function of  $\lambda$  are displayed by the curve for  $N=20$  in Figure 6 which has a sharp maximum for large pores. The position and magnitude of the maximum seem to depend on the chain length. However, a complete description of this dependence requires data of very high precision because  $K$  is a function of the difference of two large numbers in an exponent. Using our data a single curve in Figure 6 was constructed for chains with 40 and 60 segments. After reaching a maximum this curve must also drop to zero at  $\lambda=0$ .

From the data summarized in Table 1 the concentration effect can now be incorporated into the curve  $K$  vs.  $\lambda$ , which is the focus of the all theoretical treatments of partitioning. Such a plot for  $K_0$  and for  $K(0.1)$  is presented in Figure 7 and in the region of small  $\lambda$  the dramatic shift of the partition curve in favour of increased partitioning is evident. For example the partition coefficient  $K(0.1)$  determined at the concentration of 10 vol% is about 33% higher than the infinite dilution value  $K_0$  for chains with 40 segments at  $\lambda=0.25$ . As noted previously the number of segments may reflect either the chain length or the conformational flexibility of the chain. The shorter (or more rigid) chains bring about enhanced partitioning in a way similar to that caused by an increase in the bulk phase concentration.

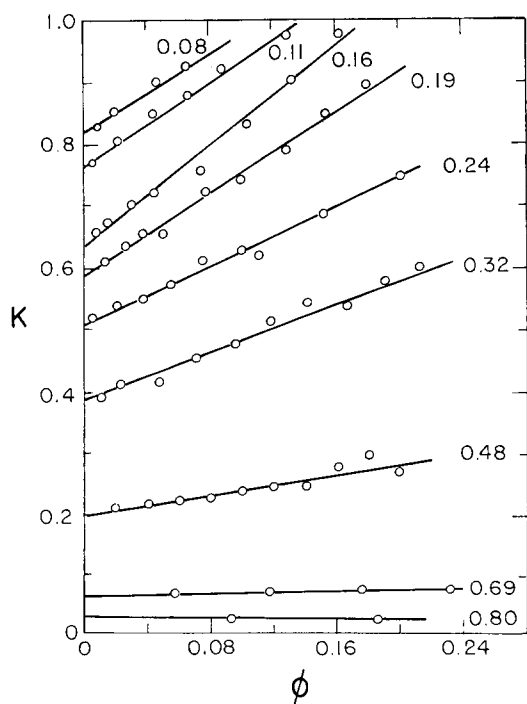


Figure 4 The partition coefficient  $K$  as a function of the bulk volume fraction  $\phi$  for chains with  $N=20$  at different values of  $\lambda$

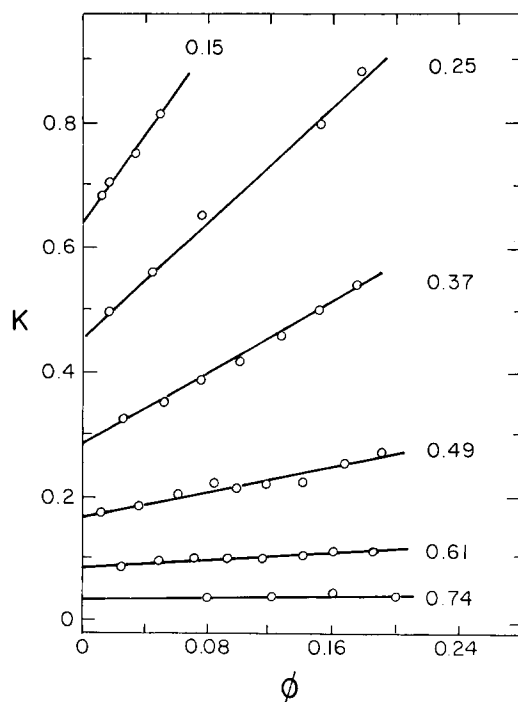


Figure 5 The partition coefficient  $K$  as a function of the bulk volume fraction  $\phi$  for chains with  $N=40$  at different values of  $\lambda$

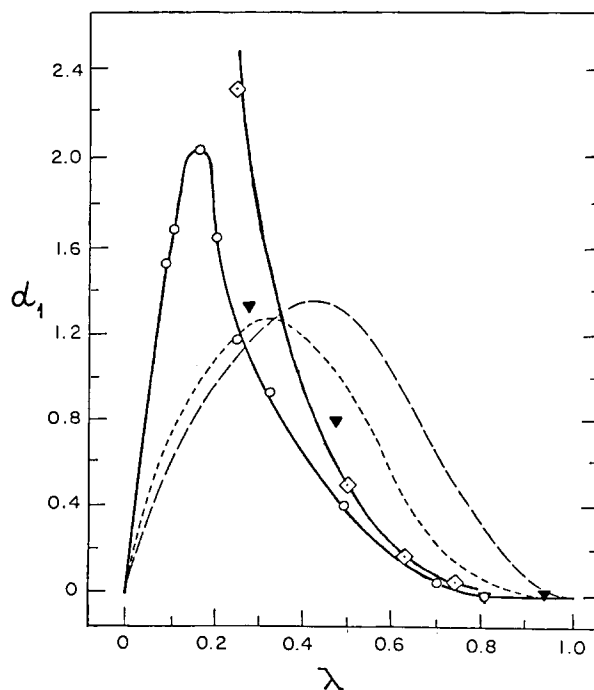
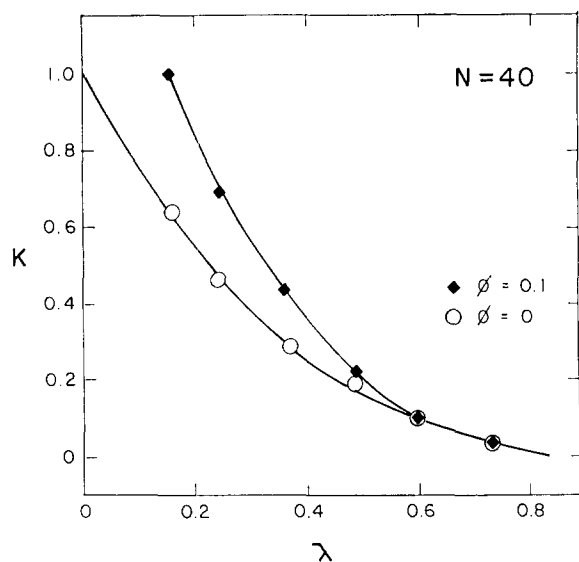


Figure 6 The dependence of the slope  $\alpha_1$  on the ratio  $\lambda$  for chains with 20 ( $\circ$ ), 40 ( $\diamond$ ) and 60 ( $\blacktriangledown$ ) segments (solid lines). The dashed lines are theoretical plots for hard sphere solutes in a spherical cavity<sup>2</sup> (---) and in a cylindrical pore<sup>6</sup> (-.-.-)

#### Comparison with analytical theories

The calculation of steric partitioning of hard-sphere solutes<sup>2,3,6</sup> is at present the only theory to which our MC results can be compared. Hence, Figure 6 also includes plots of the virial coefficient  $\alpha_1$  from equation (1) computed for spherical solutes in spherical cavities<sup>2</sup> and analogous values from the alternative theory for cylindrical pores<sup>6</sup>. Both curves show maxima at  $\lambda$  of about 0.3–0.4, i.e. for slightly larger pores than MC



**Figure 7** The partition curve  $K$  versus  $\lambda$  from simulations in an athermal system of chains with  $N=40$  at infinitely dilute system ( $K_0$ ) and at a concentration of 10 vol% ( $K(0.1)$ )

curves show for flexible chains. The computations for a spherical cavity<sup>2</sup> which resembles more closely the present cubic box pores, predict a maximum of 1.27 for  $\alpha_1$  at  $\lambda$  about 0.3.

Despite the only qualitative agreement of the curves for spherical and flexible chains in *Figure 7*, both approaches share a common origin with regards to the concentration effect, namely the existence of an enriched region of solute along the pore walls because of steric ('excluded volume') interactions of solute and pore. The 'layering' of the solute about the periphery of the pore is best demonstrated by density distribution curves computed for hard spheres in pores of various shapes<sup>2</sup> and for flexible chains in a slit<sup>22,23</sup>. By analogy with the results for spherical solutes we can expect that the layering of the chain segments along the pore walls is even more pronounced in the present case of cubic pores because of the presence of corners. The concentration of the enriched region should be greater in the corners of a box than in the centre of the faces of the box. This phenomenon was convincingly demonstrated<sup>3</sup> for spherical solutes in pores of polygonal cross section for which the concentration effect increases as the number of sides of the polygon decreases. It was emphasized<sup>3</sup> that the replacement of a pore with polygonal cross section by a tubular pore could lead to severe underestimation of the concentration effect. By analogy, the same deduction should apply when comparing the partition behaviour at finite concentration for a spherical cavity and for a cubic box.

For flexible chains, however, two additional factors, the connectivity of segments in a chain and chain compressibility, are operative in the concentration effect. The chain connectivity imposes a short-range correlation on the position of neighbouring segments and thus the thickness of the enriched layer should increase relative to the value for simple spherical molecules. The compressibility of flexible chains due both to the pore constraints (*Figure 1*) or to the concentration could be an even more important factor. The compression of the effective hydrodynamic volume with increased concentration in the bulk phase has been considered as a major factor in the

thermodynamic theory<sup>12,13</sup> of the concentration effect in gel chromatography. In gel chromatography the partition coefficient increases with column loading as the maximum of a peak shifts to higher elution volumes. The reduction of coil dimensions should be even more dramatic within pores because of the combined influence of constraints imposed by pores and by neighbouring molecules. In contrast to hard-sphere theories, the partitioning data from simulation also include the phenomenon of variable solute size during partitioning. To summarize, the comparison of the curves in *Figure 7*, the difference in the assumed shape of the pores, the chain connectivity and the compressibility of swollen coils contribute to the diversity of the curves, even if solute layering on the pore periphery is a common feature of steric partitioning of both spherical and flexible chain molecules.

#### Comparison with experimental partitioning

The effect of concentration on the partitioning of macromolecules is well documented by numerous measurements of static equilibrium in porous supports or by gel chromatography<sup>11-14,24-26</sup>. However because MC calculations on a cubic lattice do not reflect the structural details of real macromolecules, their comparison with experimental data is restricted to qualitative trends only. In addition, partitioning in the majority of experimental studies is governed not only by the steric mechanisms but also by other interactions such as solute adsorption on pore walls and electrostatic forces, which contribute to the overall partition coefficient. The complexity of pore geometry in porous supports and the frequent polydispersity of macromolecular solutes are additional factors compromising the comparison.

In qualitative terms, the results of simulations are supported by several types of experimental observations. In the majority of static and dynamic measurements<sup>11-14,23-25</sup> a linear dependence of  $K$  on the bulk concentration was observed in dilute solution (up to a concentration of several mass per cent); this function became concave only at higher concentrations. In agreement with these calculations only positive (or zero) slopes  $\alpha_1$  have been reported in the literature. The computed variation of the slope  $\alpha_1$  with  $\lambda$  has its counterpart (assuming the fixed size of pore  $a_p$ ) in the concave function  $\alpha_1$  versus molecular weight  $M$  reported from experiment<sup>14</sup>. The predictions of the hard-sphere theory have been compared to the experimental data for partitioning of dextran in equilibrium with glass porous beads in aqueous solution<sup>11</sup>. It was found that the experimental data are consistently lower, smaller by a factor of 2 or 3 than the calculated results. The maximum measured value of  $\alpha_1$  was about 0.53 and similar values were found for  $\lambda$  close to 1 where the theory predicts a negligible concentration effect. Using the concept of hard spheres, the data measured for partitioning of polystyrene with  $M_n = 6.7 \times 10^5$  in tetrahydrofuran in porous glass<sup>14</sup> were recalculated<sup>17</sup> to give 0.18 for the slope  $\alpha_1$ . Because of the factors mentioned above it is difficult to attribute this experimental value to a specific range on the curve  $K$  versus  $\lambda$ . In a rough estimation it seems that the nominal pore size (10 nm) of CPG glass used<sup>14</sup> and solute size are comparable. Thus the ratio  $\lambda$  should be well over 0.5 in the descending (to  $\lambda \rightarrow 1$ ) part of the curves in *Figure 6*.

Finally, we note the significant difference between theory and experiment which concerns solute-solvent

interactions. The presence of a solvent has not yet been explicitly accounted for in the hard sphere theory or in MC calculations. On the other hand practical considerations especially in gel chromatography, favour measurements in thermodynamically good solvents where the role of solvent-coil interactions in the concentration effect become prominent. The swelling of coils in good solvents considerably modifies their size. The gel chromatography measurements in various solvents have confirmed that the concentration effect (the slope  $\alpha_1$ ) is amplified or reduced depending on the solvent quality. The theory of the concentration effect<sup>13</sup> corroborates the experimentally found<sup>14</sup> dependence of the slope  $\alpha_1$  on the quality of solvent expressed as  $A_2M$  where  $A_2$  is the second virial coefficient of a macromolecular solute in a given solvent. In this way the theory has rationalized the concentration independent partition coefficient found for theta solvents<sup>14</sup>. In contrast, this theory<sup>13</sup>, because it is based on the compression of coil volume, predicts zero values of  $\alpha_1$  for all hard sphere solutes. Interestingly, the hard core theory<sup>6</sup> also suggests that the slope  $\alpha_1$  should be proportional to the product  $A_2M$ .

In summary, the increase in bulk concentration favours partitioning, i.e. the curve  $K$  versus  $\lambda$  is shifted to the right. Qualitatively, this shift also brings about a decrease in chain length, or an increase in chain rigidity, or attractive solute-pore interactions (adsorption)<sup>9</sup>, etc. The hard-sphere data indicate that the inclusion of electrostatic interactions should reduce the partitioning and should shift the partition curve to the left. In gel chromatography an equivalent of the curve  $K$  versus  $\lambda$  is used, called the universal calibration, which relates the elution volume to the product  $[\eta]M$  where  $[\eta]$  is the intrinsic viscosity. The product  $[\eta]M$  is proportional to the hydrodynamic volume of the solute and thus to the radius of gyration of the macromolecule and for fixed pore size  $a_p$  is also proportional to the ratio  $\lambda$ . The elution volume is a direct measure of the partition coefficient. In this way the shifts of the theoretically computed partition curves  $K$  versus  $\lambda$  can be related to the shifts of universal calibration curves which are well documented by experiment especially with respect to the solute concentration and solute adsorption<sup>12,27</sup>.

#### Implications for hindered transport

The effect of concentration on partitioning is of direct relevance to the hindered transport of flexible macromolecules in porous materials. The apparent diffusion coefficient  $D$  of a solute in a pore is much smaller than the coefficient  $D_\infty$  in bulk solution. Similarly, during ultrafiltration through a membrane convective transport is restricted by pore walls. The fraction of solute rejected by a membrane,  $\sigma$ , is denoted as the reflection coefficient. The two types of transport parameter  $D/D_\infty$  and  $\sigma$  are related to the partition coefficient  $K$ . For hindered diffusion, the relation  $D/D_\infty = K\kappa^{-1}$  is valid, where  $\kappa^{-1}$ , the inverse enhanced drag or ratio of friction coefficient of the solute to that within a pore, can be readily evaluated for some simple configurations<sup>28</sup>. It should be noted in this context that recently a new direct measurement of the coefficient  $D$  inside pores was reported<sup>29,30</sup> based on quasi-elastic light scattering. This technique does not require the knowledge of the partition coefficient  $K$  to evaluate the coefficient  $D$  because it explores directly the movement of solute within the pore medium. However, phenomenological methods<sup>15,28</sup> still prevail in

the determination of the coefficient  $D$  by determining the ratio of  $D/D_\infty$  which require knowledge of the coefficient  $K$ . In ultrafiltration, the reflection coefficient  $\sigma$  is a function of hydrodynamic interactions and of the partition coefficient  $K$ . For the simplest case of steric interactions of hard sphere with a cylindrical pore, the simple relation  $\sigma = (1 - K)^2$  applies<sup>16,28</sup>.

Because of an intimate connection between hindered transport and partitioning it is obvious that any concentration dependence of  $K$  will affect the ratio  $D/D_\infty$  and/or the coefficient  $\sigma$ . For hard spheres in cylindrical pores experimental and theoretical results<sup>7,31</sup> have shown a reduction of  $\sigma$  with concentration. Measurements of hindered transport of flexible polymers are usually performed at finite concentrations, however, the concentration effect is frequently overlooked and only in a few cases has been investigated<sup>15,16</sup>. The scaling theory applied to rationalize these measurements<sup>15,16</sup> does not provide the numerical prefactors; in addition, the theory is apparently restricted only to the range of comparable sizes of coils and pores whereas the partitioning occurs when the coil size is smaller than the pore size. The concentration effect in hindered transport should be governed by the same mechanisms as discussed above for partitioning with suitable modifications for the superimposed hydrodynamic interactions of solute-wall and solute-solute.

## CONCLUSIONS

Simulations in an athermal system have confirmed the linear dependence of the partition coefficient  $K$  on bulk concentration. In the range of small coil-to-pore size ratio  $\lambda$  this effect dramatically enhances the partition. The origin of the effect derives from the formation of an enriched region of segments on the periphery of the pore walls which has already been described for hard-sphere solutes and amended in the case of flexible chains because of their connectivity and compressibility. This type of concentration effect complicated by hydrodynamic interactions also operates for the hindered transport of flexible molecules at finite concentrations.

## ACKNOWLEDGEMENT

This work was supported in part by a grant from AFOSR, #88-011.

## REFERENCES

- Giddings, J. C., Kucera, E., Russell, C. P. and Myers, M. N. *J. Phys. Chem.* 1968, **72**, 4397
- Glandt, D. E. *AIChE J.* 1981, **27**, 51
- Glandt, D. E. *J. Membr. Sci.* 1981, **8**, 331
- Casassa, E. F. *J. Polym. Sci. B* 1967, **5**, 773
- Casassa, E. F. and Tagami, Y. *Macromolecules* 1969, **2**, 14
- Anderson, J. L. and Brannon, J. H. *J. Polym. Sci., Polym. Phys. Edn.* 1981, **19**, 405
- Mitchel, B. D. and Dean, W. M. *J. Coll. Int. Sci.* 1986, **113**, 132
- Dayantis, J. and Sturm, J. *Polymer* 1985, **26**, 1631
- Davidson, M. G., Suter, U. W. and Deen, W. M. *Macromolecules* 1987, **20**, 1141
- Cifra, P., Bleha, T. and Romanov, A. *Polymer* 1988, **29**, 1664
- Brannon, J. H. and Anderson, J. L. *J. Polym. Sci., Polym. Phys. Edn.* 1982, **20**, 857
- Rudin, A. and Wagner, R. A. *J. Appl. Polym. Sci.* 1976, **20**, 1483
- Bleha, T., Mlynek, J. and Berek, D. *Polymer* 1980, **21**, 798
- Bleha, T., Spychaj, T., Vondra, R. and Berek, D. *J. Polym. Sci., Polym. Phys. Edn.* 1983, **21**, 1903

- 15 Guillot, G., Leger, L. and Rondelez, F. *Macromolecules* 1985, **18**, 2531
- 16 Long, T. D. and Anderson, J. L. *J. Polym. Sci., Polym. Phys. Edn.* 1984, **22**, 1261
- 17 Cifra, P., Bleha, T. and Romanov, A. *Makromol. Chem., Rapid Commun.* 1988, **9**, 355
- 18 Meirovitch, J. *J. Chem. Phys.* 1983, **79**, 502
- 19 Okamoto, H. *J. Chem. Phys.* 1983, **79**, 3976
- 20 McCrackin, F. L., Mazur, J. and Guttman, Ch. *Macromolecules* 1977, **6**, 859
- 21 Yamakawa, H. 'Modern Theory of Polymer Solution', Harper and Row, New York (1971)
- 22 Ishinabe, T. *J. Chem. Phys.* 1985, **83**, 423
- 23 Madden, W. G. *J. Chem. Phys.* 1987, **87**, 1405
- 24 Janca, J., Pokorný, S., Bleha, M. and Chiantore, O. *J. Liq. Chromatogr.* 1980, **3**, 953
- 25 Tejero, R., Soria, V., Campos, A., Figueruelo, J. E. and Abad, C. *J. Liq. Chromatogr.* 1986, **9**, 711
- 26 Chiantore, O. and Guaita, M. *J. Liq. Chromatogr.* 1985, **8**, 1453
- 27 Bakos, D., Bleha, T., Ozima, A. and Berek, D. *J. Appl. Polym. Sci.* 1979, **23**, 2233
- 28 Dean, W. M. *AIChE J.* 1987, **33**, 1409
- 29 Bishop, M. T., Langley, K. H. and Karasz, F. E. *Phys. Rev. Lett.* 1986, **57**, 1741
- 30 Bishop, M. T., Langley, K. H. and Karasz, F. E. *Macromolecules* 1989, **22**, 1220
- 31 Adamski, R. P. and Anderson, J. L. *Biophys. J.* 1983, **44**, 79